JOURNAL OF CATALYSIS **15**, 107–119 (1989)

An Infrared Study of the Influence of CO Adsorption on the Topology of Supported Ruthenium

FRIGYES SOLYMOSI AND JÁNOS RASKÓ

Reaction Kinetics Research Group of the Hungarian Academy of Sciences and Institute of Solid State and Radiochemistry, University of Szeged, P.O. Box 105, H-6701 Szeged, Hungary

Received March 21, 1988; revised May 31, 1988

The interaction of CO with alumina-supported ruthenium, reduced at different temperatures, was investigated by following the development of infrared bands due to adsorbed CO. It was concluded that the adsorption of CO on Ru at 170–350 K leads to the oxidative disruption of Ru clusters as indicated by the slow transformation of the band at 2020–2040 cm^{-1} due to Ru_x–CO to bands at 2140 and 2075 cm^{-1} attributed to $Ru^{n+}(CO)_2$ species (n = 1–3). This process occurred more slowly under dry conditions, and in the presence of hydrogen, whereas it was accelerated by H_2O addition. Analysis of spectral features suggested the involvement of the isolated OH groups on the alumina support in the oxidative disruption process. It was demonstrated that at higher temperatures, namely at around 500 K, the presence of CO causes the reductive agglomeration of Ru^{n+} sites, i.e., the reformation of Ru_x clusters. © 1989 Academic Press, Inc.

INTRODUCTION

The effects of the physical and chemical properties of solids on the coordination, structure, and bonding of adsorbed species have been extensively investigated by different spectroscopic methods. However, relatively little attention has been paid so far to the fact that, due to the strong interaction of gases with metals, the state and surface morphology of metal crystallites can also be influenced, which may alter the adsorptive properties of the metals and thereby the infrared spectrum of the adsorbed gases. The chemisorption of gas molecules on highly dispersed supported metals at room temperature is considered to be a fast process, and therefore no significant spectral changes are expected after an extended adsorption time. The absence of time-dependent spectral changes obviously does not mean that the adsorption of gases exerts no influence on the structure of supported metals: depending on the nature of the metal and on its crystallite size, this process could also occur very rapidly at around room temperature.

However, if the metal crystallites are larger, the effect of gases occurs more slowly or, at least, can be detected only after a prolonged reaction time. This was demonstrated by Solymosi and Pásztor (*1, 2*) in the case of Rh/Al_2O_3 reduced at 1173 K. The adsorption of CO on this sample produced only bands due to Rh_x–CO and $\begin{smallmatrix}\mathrm{Rh}\\ \mathrm{Rh}\end{smallmatrix}\!>\!\mathrm{CO}$ species, but after several hours the characteristic bands of gem-dicarbonyl, $\mathrm{Rh}^{\mathrm{I}}\!<\!\begin{smallmatrix}\mathrm{CO}\\ \mathrm{CO}\end{smallmatrix}$, appeared and grew in intensity with increasing adsorption time. This was explained by a CO-induced oxidative disruption of Rh crystallites to Rh^I sites on which CO binds in the form of gem-dicarbonyl (*3–5*). The presence of H_2O facilitated this process (*1*), whereas that of H_2 hindered it (*2*). It was also shown that at higher temperatures, above 423 K, the effect of CO adsorption is different: in this case it promoted the reductive agglomeration of isolated Rh^I sites (*1*), which was further accelerated by adding H_2 to the CO (*2*).

Direct evidence for the disruption of Rh

0021-9517/89 $3.00

crystallites was provided by previous EXAFS results (*6–8*), which showed that the adsorption of CO at 300 K significantly perturbs the local coordination environment of the Rh_x clusters. However, the clear establishment of this effect by EXAFS required an initially highly dispersed system (low Rh content, viz. 0.5%, and low reduction temperature, ~573 K) and a significant extent of Rh–Rh disruption. Further details on the CO-induced structural changes in supported Rh were obtained by infrared spectroscopy (*9–17*). The effects of several factors have been established, namely the effects of supports (*9–11*) and additives (*11, 12*) of the presence of H_2 (*2, 17*), O_2 (*13, 17*), and NO (*13*), and of the role of OH groups on the supports (*14*). Furthermore, the structural changes in Rh were also examined during catalytic reactions: H_2 + CO (*17*), H_2 + CO_2 (*15*), and NO + CO (*16*).

In the present study, an attempt is made to establish whether CO adsorption exerts a similar influence on the topology of another supported noble metal. For this purpose we chose Ru, on which the adsorption of CO produces three absorption bands in the IR spectrum, at 1990–2030, 2060–2080, and 2120 cm^{-1} (*18–36*). For convenience, the bands are referred to as low-, medium-, and high-frequency bands, denoted LF, MF, and HF. Although the positions of these bands agreed quite well in different studies, their assignment is still a matter of controversy. We return to this point under Discussion.

EXPERIMENTAL

IR spectra were recorded with a Specord 75 IR double-beam spectrometer (Zeiss, Jena) with a resolution of ±5 cm^{-1}. The cell used was suitable for recording the spectra at low and high temperatures. The cell was connected to a vacuum line and to a closed circulation system in which the gases were circulated during adsorption by a small magnetic pump.

Ru/Al_2O_3 samples were prepared by incipient wetting of Al_2O_3 (Degussa, BET area 100 m^2/g) with an aqueous solution of $RuCl_3 \cdot H_2O$. After impregnation, the samples were dried in air at 330 K.

For the IR studies, the dried Ru/Al_2O_3 powder was pressed into thin self-supporting wafers (30 × 10 mm, 20 mg/cm^2). The pretreatment of the samples was performed in the vacuum IR cell: the samples were (a) heated (20 K min^{-1}) to 573 K under constant evacuation, (b) oxidized with 100 Torr O_2 (1 Torr = 133.3 Pa) for 60 min at 573 K, (c) evacuated for 30 min, and (d) reduced with 100 Torr H_2 for 60 min at 573–773 K. This was followed by degassing at the same temperature for 30 min and by cooling the sample to the temperature of the experiment. The gases were circulated during the oxidation and reduction processes.

The gases used were of commercial purity. CO (99.9%) was purified by bubbling through a $Mn(OH)_2$ suspension. Water vapor was frozen out by a trap cooled with a dry ice–acetone mixture. The dispersion of supported Ru reduced at different temperatures has been determined by H_2 adsorption at 300 K (*21, 22*). Data obtained are shown in Table 1.

RESULTS

1. Adsorption of CO at 260–383 K

As regards the assignment of the absorption bands of CO on supported Ru, there is general agreement that the LF band at 1990–2030 cm^{-1} corresponds to the vibration of CO linearly bonded on Ru crystallites (*18–31*). In the first part of our experiments, our goal was to prepare Ru crystallites on which the adsorption of CO produces only the LF band or, at least, the intensities of the other two bands are minimal. In the case of Rh/Al_2O_3, this was achieved by using a larger amount of metal and/or a higher reduction temperature (*1*).

Figure 1 shows the effect of the temperature of reduction of 5% Ru/Al_2O_3 on the IR

TABLE 1

Adsorption of H_2 on Ru/Al_2O_3 at 300 K

Sample	Reduction temp. (K)	H/Ru
5% Ru/Al_2C_3	573	19
	673	14
	773	6
1% Ru/Al_2O_3	573	26[a]
	673	20

[a] This high value for H/Ru may indicate that a fraction of hydrogen spilt over onto the alumina support.

spectrum of adsorbed CO. If we applied a low pressure of CO, the dominant absorption band at 300 K was at 2025 cm^{-1} for the sample reduced at 573 K. However, weak bands can also be seen at 2140 cm^{-1} (HF band) and 2075 cm^{-1} (MF band). The initial intensities of these bands were clearly less at lower temperature, 260 K, but higher at 373 K. When the reduction temperature was raised, the intensity of the LF band was somewhat less and the other weak bands were missing or were very weak in the spectra taken 5 min after CO introduction at 300 K.

After an extended adsorption time, however, the HF and MF bands grew in intensity, or, if they were initially absent (R_T = 823 K), they slowly developed. The production of these spectral changes for the samples reduced at higher temperatures required a higher pressure of CO (Figs. 2–4). These spectral changes also occurred at a higher adsorption temperature, 383 K, where after adsorption for 18 h the intensities of the HF and MF bands were commensurable with that of the LF band (Fig. 3). It is important to note that the development of the HF and MF bands at 383 K is clearly accompanied by a decrease in intensity of the LF band and by its shift to lower frequencies. This shift is very probably a result of a lower concentration of linearly bonded CO attached to Ru_x and of the reduced extent of dipole–dipole coupling. This process also occurs at 423 K, but the bands at 2075 and 2140 cm^{-1} are then much weaker than those at 383 K.

2. *Adsorption of CO at 448–548 K*

In the case of Rh/Al_2O_3 we observed that at higher temperatures, above 423 K, the presence of CO caused the reductive agglomeration of Rh^I sites which was indicated by a decrease in gem-dicarbonyl and by a simultaneous formation of Rh_x–CO species.

In the present case the situation is more complex, as the HF and MF bands (tentatively attributed to CO bonded to partially oxidized Ru) cannot be produced without the appearance of the LF band, even when a smaller amount of Ru and a lower reduction temperature are applied. Significant in-

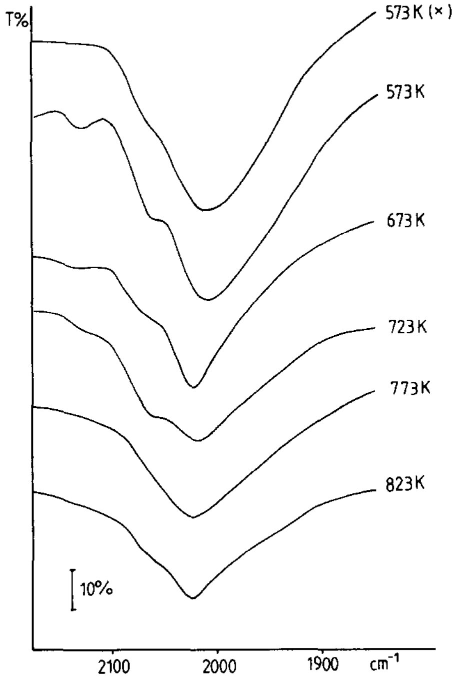

FIG. 1. Infrared spectra of adsorbed CO as a function of reduction temperature of 5% Ru/Al_2O_3 in the presence of 0.5 Torr of CO. The reduction temperature of the sample is shown on the spectra. Spectra were taken at 300 K (5 min after CO introduction) with the exception of spectrum (×) where the adsorption temperature was 260 K.

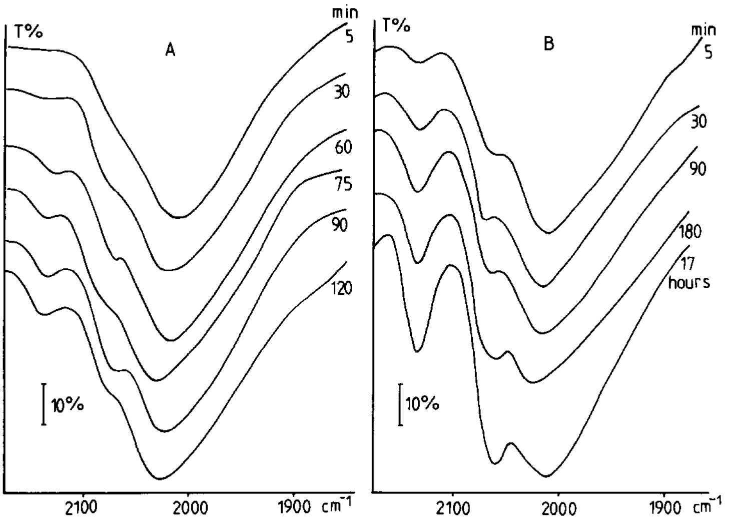

FIG. 2. Changes in the infrared spectrum of adsorbed CO on 5% Ru/Al_2O_3 (R_T = 573 K) in the presence of 0.5 Torr of CO as a function of time at 300 K (A) and 383 K (B).

tensities of the HF and MF bands were achieved through prolonged contact of Ru/Al_2O_3 (R_T = 573 K) with CO containing 1 Torr of H_2O. As shown by the spectra displayed in Fig. 5, no significant spectral changes occurred after the 1% Ru/Al_2O_3 sample was heated in the presence of 50 Torr of CO to 448 K and kept there for several hours. A more appreciable attenuation of the HF and MF bands was experienced at 498 K, and particularly at 548 K. However, this change was not accompanied by an intensification of the LF band; indeed, its intensity even decayed at these temperatures. In other words, the relative intensities of the three bands remained practically the same. When the sample was cooled in CO gas at room temperature, an enhancement of all bands occurred, but the original intensities were not attained in 15 min.

Similar measurements were performed

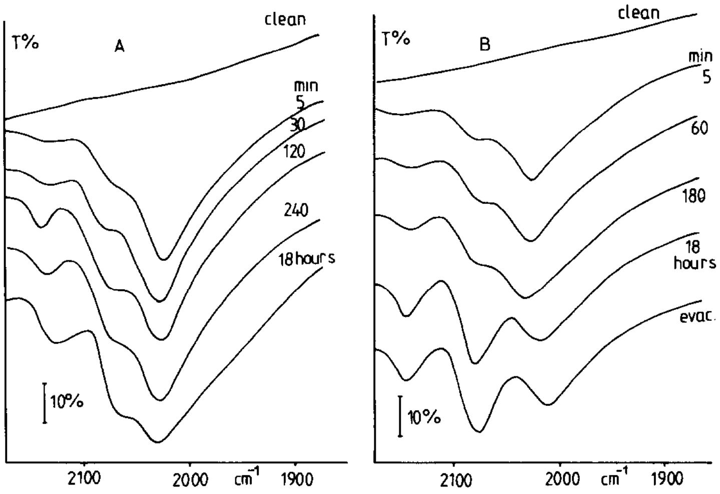

FIG. 3. Changes in the infrared spectrum of adsorbed CO on 5% Ru/Al_2O_3 (R_T = 673 K) in the presence of 0.5 Torr of CO as a function of time at 300 K (A) and 383 K (B).

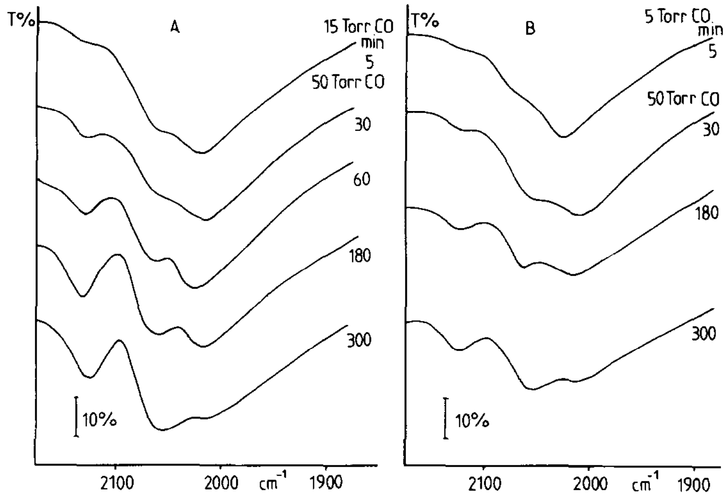

FIG. 4. Changes in the infrared spectra of adsorbed CO on 5% Ru/Al_2O_3 reduced at 723 K (A) and 773 K (B) in the presence of CO as a function of time at 300 K.

with 5% Ru/Al_2O_3 (R_T = 573 K). Characteristic spectra are presented in Fig. 6. In this case a well-observable decay occurred in the HF and MF bands even at 448 K, which was apparently accompanied by a slight intensification of the LF band. This feature was more pronounced at 498 and 548 K.

3. *Effects of H_2O and H_2 on CO-Induced Spectral Changes*

In the subsequent measurements we examined the effects of H_2O and H_2 on the spectral changes observed following CO adsorption at different temperatures. As

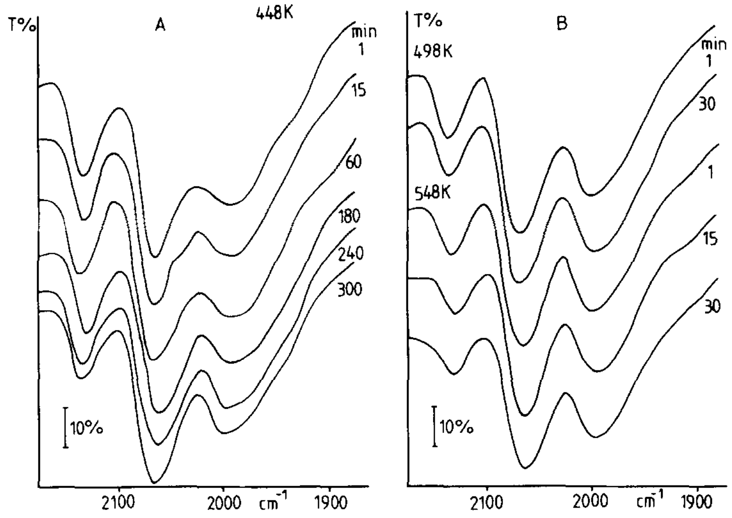

FIG. 5. Changes in the infrared spectrum of 1% Ru/Al_2O_3 (R_T = 573 K) in the presence of 50 Torr of CO at 448, 498, and 548 K. The sample was kept in 50 Torr of CO containing 0.5 Torr of H_2O at 300 K for 3 h. Afterward the gas phase was changed to pure CO and the sample was quickly heated, first to 448, then 498, and finally 548 K.

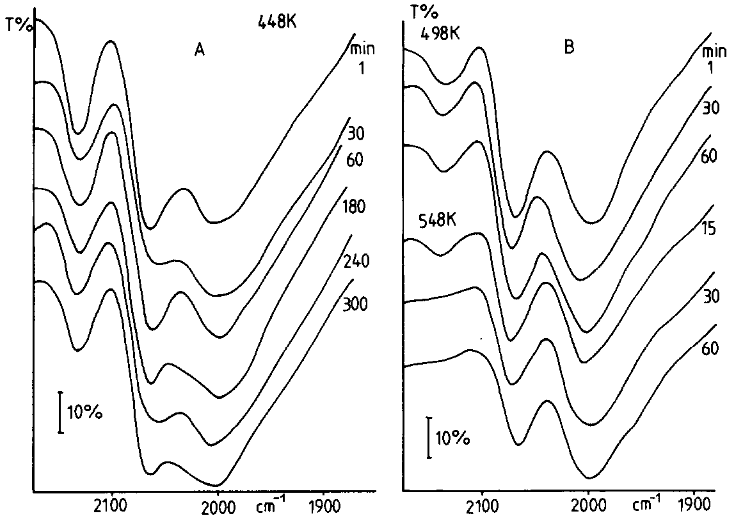

FIG. 6. Changes in the infrared spectrum of 5% Ru/Al_2O_3 (R_T = 573 K) in the presence of 5 Torr of CO at 448, 498, and 548 K. For further details, see the legend of Fig. 5.

seen in Fig. 7, the presence of H_2O accelerated the development of the HF and MF bands at 300 K and this effect was more pronounced when the spectral changes were compared with those observed under very dry conditions (preparation of Ru/Al_2O_3 in methanol, and performance of all manipulations under the driest possible conditions).

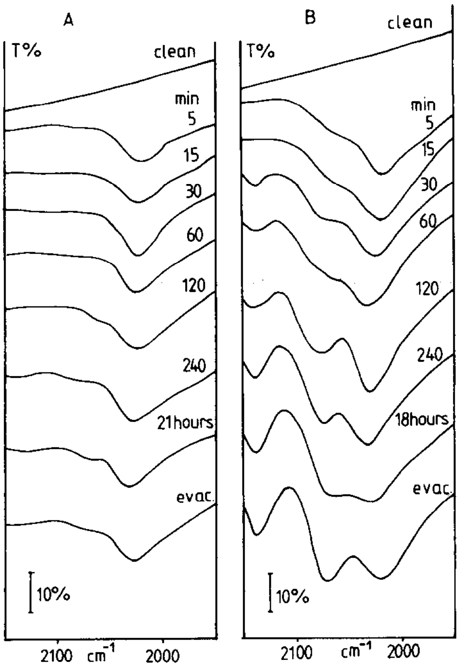

FIG. 7. Effect of H_2O (0.1 Torr) on the spectral changes observed for 5% Ru/AlO_3 (R_T = 673 K) in the presence of 0.5 Torr of CO at 300 K. (A) Under dry conditions; (B) in the presence of 0.1 Torr of H_2O.

The development of HF and MF bands was practically not influenced by the presence of H_2 (5 Torr of CO + 100 Torr of H_2) at 300 K. However, it prevented or considerably slowed the development of these absorption bands at 373 K. This was particularly the case at higher H_2 pressure (Fig. 8). When the HF and MF bands were already formed by CO adsorption alone, the subsequent admission of the H_2 on the degassed sample caused only a very slow attention of HF and MF bands at 300–373 K. However, the addition of H_2 to CO significantly increased the elimination of HF and MF bands observed in the presence of the CO above 448 K and intensified the LF band of CO.

In order to obtain spectroscopic evidence for the involvement of OH groups on Al_2O_3 in the formation of the HF and MF bands during CO adsorption some preliminary measurements were also performed in the ν_{OH} region of the IR spectrum of Ru/Al_2O_3. For this purpose we chose the 5% Ru/

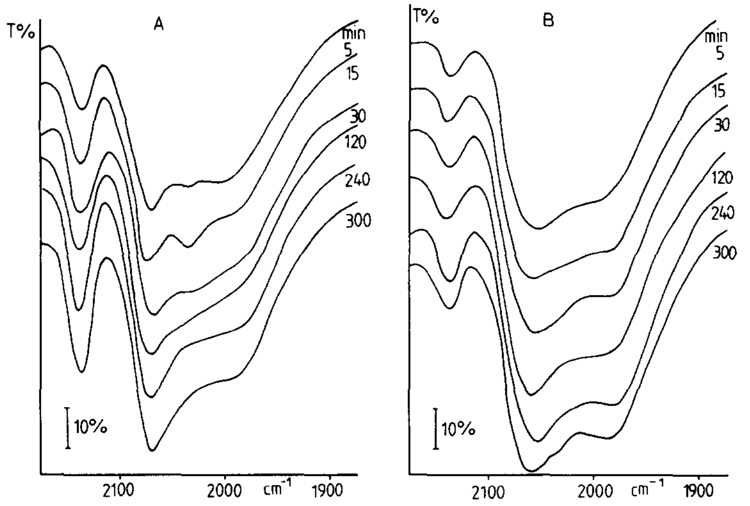

FIG. 8. Effect of H_2 on the spectral changes observed for 1% Ru/Al_2O_3 (R_T = 573 K) at 373 K in the presence of 5 Torr of CO. Pressure of H_2: (A) 0 Torr, (B) 100 Torr.

Al_2O_3 sample (R_T = 773 K). In the spectrum of reduced Ru/Al_2O_3 a broad feature was seen at around 3550 cm^{-1}, which is probably due to H-bonded OH on alumina (*37*, *38*). Furthermore, two very small shoulders can be identified at 3735 and 3679 cm^{-1}, which were assigned to isolated surface OH groups (*37*, *38*). Perturbations of these OH groups were experienced in the case of Rh/Al_2O_3 with increasing CO coverage (*14*).

As the bands due to isolated OH groups are extremely weak their perturbations can be detected only in the difference spectra obtained by subtracting the background spectrum from each subsequent spectrum taken after CO absorption. As shown in Fig. 9, an attenuation of the band at 3750 cm^{-1} (exhibited in the form of a sharp negative peak in the difference spectra) occurs as the pressure of CO is increased for Ru/Al_2O_3 (R_T = 773 K) suggesting the depletion of isolated OH groups from the support sur-

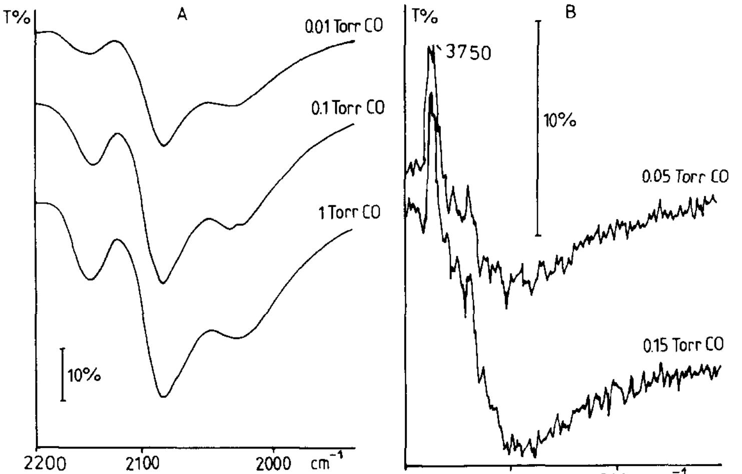

FIG. 9. (A) Infrared spectra of 5% Ru/Al_2O_3 (R_T = 773 K) following CO adsorption at 300 K. (B) Difference spectra in the ν_{OH} region. Adsorption time of CO was 30 min.

face as the HF and MF bands of adsorbed CO on reduced Ru are being developed. No change was detected yet in the intensity of the band at 3679 cm^{-1}. Further investigations are in progress to follow the depletion and intensification of the bands for isolated OH groups on supported Ru under different conditions (*39*).

DISCUSSION

1. Previous Spectral Assignments

The adsorption of CO on supported Ru has been extensively studied by means of IR spectroscopy (*18–36*). Before interpretation of our experimental results, it seems worthwhile to summarize the main points of the results and the different models suggested. Whereas the results in the literature agree quite well that three absorption bands (at 1990–2030, 2080, and 2140 cm^{-1}) dominate the spectrum above 2000 cm^{-1}, opinions differ widely as regards the assignments of these bands. Several authors (*23, 24*) have assumed a multiple adsorption of CO on coordinatively unsaturated Ru sites, which seems to be in harmony with the measured CO/H uptake ratio. Dalla Betta (*20*) observed that the particle size of Ru on Al_2O_3 has a profound effect on the positions of the CO bands in the spectra. The band at ca. 2030 cm^{-1} for a sample with an average particle size greater than 90 Å was attributed to CO adsorbed on low-index planes of Ru, while the bands at 2140 and 2080 cm^{-1} (for a sample with a particle size of 60 Å or less) were associated with CO adsorbed on low coordination edge and corner metal atoms with more than one adsorbed CO.

From the data obtained on reduced and oxidized Ru/SiO_2, Brown and Gonzalez (*25*) concluded that the band at 2030 cm^{-1} is due to the vibration of CO linearly bonded to Ru_x, while the HF and MF bands at 2135 and 2080 cm^{-1} are due to the vibration of CO adsorbed on a surface oxide and on a Ru atom perturbed by a nearby O atom, respectively.

Davydov and Bell (*27*) assigned a single band at 2040 cm^{-1}, produced on a fully reduced Ru/SiO_2, to linearly bonded CO. The pair of bands at 2130 and 2070 cm^{-1}, formed following CO adsorption on an oxidized sample, was assigned to the symmetric and asymmetric stretches of two CO molecules in gem-dicarbonyl, $Ru^{I}(CO)_2$. This is a species similar to that identified in the case of the CO–Rh system (*1–17*). This assignment and the formation of gem-dicarbonyl has been accepted by several authors (*21, 28–30, 32–36*).

Chen *et al.* (*31*) also observed three bands (at 2030, 2080, and 2140 cm^{-1}) during CO adsorption on reduced Ru/SiO_2. Although in their experiments the 2140 and 2080 cm^{-1} bands always appeared together, the intensity ratio was found to vary. Isotopically mixed CO adsorption suggested that these bands are due to different adsorbed species. They concluded that none of the above models, i.e., a multiple coordination model (*23, 24*), an oxidation state model (*25–27*), or a particle size model (*20*), is entirely satisfactory. They were of the opinion that the coadsorbed species can significantly alter the bonding of CO to Ru. The broadband at 2030 cm^{-1}, observed when CO was adsorbed alone on a reduced surface, was assigned to $Ru(CO)_n$ ($n \geqq 1$); the 2080 cm^{-1} band to $Ru(CO)X_m$; and the 2140 cm^{-1} band to $Ru(CO)_nX_m$, where X represents coadsorbed H_2O (or OH), O, or Cl species.

On the other hand Zecchina *et al.* (*32–34*) found that during decarbonylation of adsorbed $Ru_3(CO)_{12}$ on alumina several pairs of adsorption bands appear in the infrared spectrum which were attributed to complexes of similar structure schematically represented by the formula $(L)_yRu(CO)_2$, where L is a surface ligand and ruthenium is in different oxidation states. This assignment has been confirmed by means of ^{13}CO isotopic substitution (*33*). The pair of bands at 2138 and 2075 cm^{-1} was assigned to $Ru(CO)_2$ species in which the oxidation state of Ru was assumed to be 3. The following structure was proposed for this species,

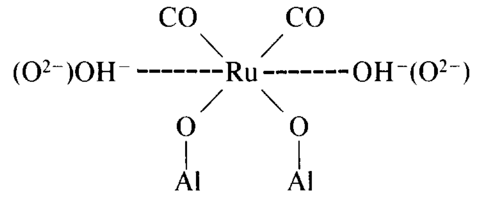

where the octahedral sphere contains $(OH)^-$ and/or O^{2-} surface ligands (*33*). It is important to point out that a similar pair of bands was produced by CO adsorption on unsaturated, CO-free Ru obtained by full decarbonylation of the $Ru_3(CO)_{12}/Al_2O_3$ system (*33*, *34*).

2. *Oxidative Disruption of Ru_x Crystallites*

A firm basis for the discussion of the spectral changes observed in the interaction of CO with Ru crystallites is that the LF band at 1990–2030 cm^{-1} is due to the vibration of CO bonded to Ru_x cluster. This state was achieved by applying a larger amount of Ru and by reducing the sample at or above 673 K under dry conditions. In this case the other adsorption centers were few in number or were not present in a concentration detectable via CO adsorption. However, the fact that the MF and HF bands did develop slowly after a long adsorption time and with the accompaniment of an attenuation of the Ru_x–CO band suggests that the CO caused the topology of the Ru crystallites to undergo a significant alteration, and that other adsorption centers were formed at the expense of Ru_x. As a working hypothesis, we may assume that the formation of a strong bond between Ru_x and CO results in a disruption of the Ru–Ru bond and in the formation of Ru centers on which CO adsorbs in different forms. The driving force behind the disruption of the Ru–Ru bonds is the high bond energy of Ru–CO, similar to that proposed for the CO-induced disruption or Rh–Rh bonds (*6*, *7*). Assuming that the adsorption of CO is fast on all Ru centers at 300 K, the results presented demonstrate that the rate of disruption increased to 383 K, but above this temperature it became very limited again. This feature cannot be attributed to a weaker adsorption of CO to the Ru_x clusters above 383 K as the Ru_x–CO band at 448–498 K is as intense as that at 383 K. It is more likely that at higher temperatures another, basically different, effect of CO comes into prominence, and this is the subject of the following section.

Although the intensities of the HF and MF bands differ greatly it is important to point out that they appear almost simultaneously. In certain cases, however, when the MF band was weak, it was not possible to see the less intense HF band in the ordinary spectrum. However, even in these cases its presence can be established in the magnified difference spectra. This observation supports the idea that the formation of surface species yielding these absorption bands is in some way connected with the same surface centers; for instance, the CO molecules adsorb on the same Ru site to yield $Ru(CO)_2$, or they are different, but the formation is connected with same surface process. *In the present case this process could be the oxidative disruption of Ru_x crystallites.* The fact that the above spectral changes occur markedly more slowly when Ru/Al_2O_3 samples are reduced at higher temperatures, which results in larger Ru particles (Fig. 4), is in harmony with the above model, as the oxidative disruption of larger Ru crystallites is obviously more restricted.

As demonstrated in Fig. 7, the spectral changes attributed to the effect of CO occurred more slowly when the sample was prepared under dry conditions. On the other hand the admission of H_2O vapor into the cell during CO adsorption clearly exerted a promoter influence on the disrupting effect of CO. In contrast, the presence of H_2 significantly hindered the development of the HF and MF bands (Fig. 8). All these features suggest the view that in addition to the disruption an oxidative process also occurs during CO adsorption, resulting very probably in Ru^I or the more stable Ru^{III} state.

The involvement of the OH groups on the alumina in the CO-induced structural changes of the Ru_x is clearly exhibited by the spectra presented in Fig. 9, where the development of HF and MF bands of adsorbed CO on Ru was accompanied by a decay in the intensity of isolated OH groups on alumina support. We note here that a direct correlation between the depletion of OH groups and the development of gem-dicarbonyl was found for Rh/Al_2O_3 by Basu *et al.* (*14*) indicating the direct participation of OH groups in the CO-induced oxidative disruption of Ru_x clusters. Although the present system seems more complicated than Rh/Al_2O_3 and the results obtained so far are not sufficient to establish the above-mentioned correlation, it appears that the adsorption of the CO induces processes on Ru/Al_2O_3 similar to those on Rh/Al_2O_3. The active OH groups are in both cases the isolated OH species; the H-bonded OH groups appear to be inactive in this reaction. This is in harmony with the general behavior of OH groups on Al_2O_3, where, depending on the geometrical configuration and the charges, the reactivity of the OH groups are expected to be different (*37, 38*).

Taking all these features into account, we suggest the following sequences for the oxidative disruption of Ru_x crystallites,

$$Ru_x + 2CO = Ru_{x-1}—CO + Ru^0—CO$$

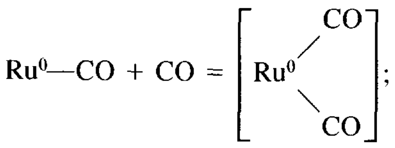

$$Ru^0—CO + CO = \left[Ru^0 \begin{matrix} CO \\ CO \end{matrix} \right];$$

[ ] = transitory species

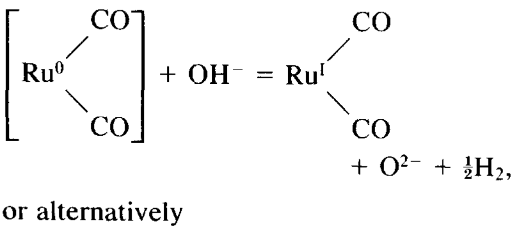

$$\left[Ru^0 \begin{matrix} CO \\ CO \end{matrix} \right] + OH^- = Ru^I \begin{matrix} CO \\ CO \end{matrix} + O^{2-} + \tfrac{1}{2}H_2,$$

or alternatively

$$2Ru + CO + 2AlOH \rightarrow 2Al—O—Ru(CO)_2 + H_2$$

or

$$Ru + CO + 2AlOH \rightarrow$$

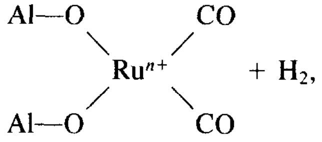

$$\begin{matrix} Al—O \\ Al—O \end{matrix} Ru^{n+} \begin{matrix} CO \\ CO \end{matrix} + H_2,$$

where n is 2, or >2 in the presence of other ligands such as O^{2-} or OH. This reaction scheme is basically the same as that proposed for the interaction of CO with Rh/Al_2O_3 (*1, 2, 6*), which was accepted with minor alteration in subsequent work (*14–17*). It differs from the view of other authors (*3, 7–9*), who described the oxidative disruption of Rh_x crystallites via CO dissociation. This latter route, however, seems totally unlikely, as the detectable dissociation of CO on supported Rh proceeds only above 473 K (*40, 41*), whereas the formation of gem-dicarbonyl occurs at slightly above 120 K (*3, 14, 17*).

The situation might be different for Ru/Al_2O_3, where according to the theoretical considerations of Broden *et al.* (*42*) and the experimental results of Kobori *et al.* (*43*), the dissociation of CO occurs more easily than on Rh/Al_2O_3. Consequently the dissociation of CO and the subsequent oxidation by adsorbed oxygen formed can also contribute to the formation of Rh^{n+} sites. As the oxygen is bonded very strongly to Ru, we can expect that the adsorbed oxygen (for the same reason as the adsorbed CO) can also induce the disruption of the Ru crystallites. Thus, we can reckon with the reaction steps

$$Ru_x + CO = Ru_x—CO$$

$$Ru_x—CO = Ru_{x-y}—C + Ru_y—O$$

$$2Ru_x—O = Ru_{2x-1}—O + Ru^0—O$$

$$Ru^0—O = Ru^+—O^-$$

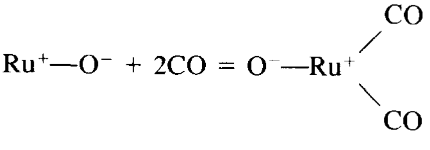

$$Ru^+—O^- + 2CO = O^-—Ru^+ \begin{matrix} CO \\ CO \end{matrix}$$

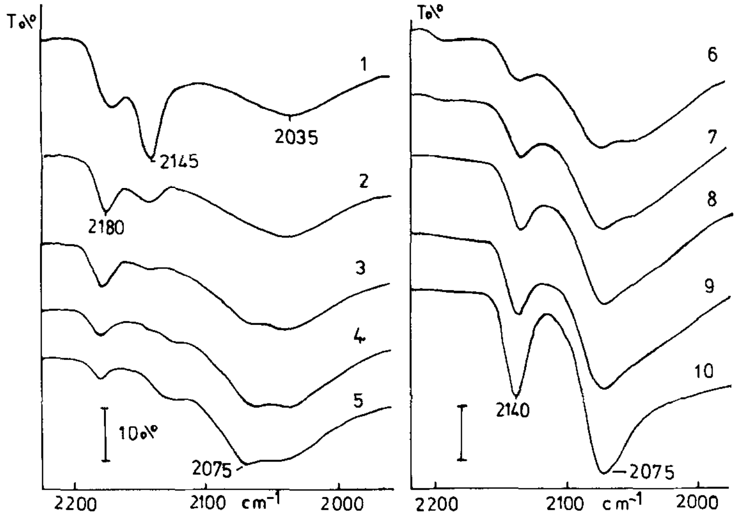

FIG. 10. Infrared spectra of CO adsorbed on 1% Ru/Al_2O_3 (R_T = 673 K). Spectra were taken after *in situ* exposure to 50 Torr of CO at 120 K (5 min) and during gradual warming of the sample to higher temperatures. 1, 120 K; 2, 150 K; 3, 170 K; 4, 210 K; 5, 222 K; 6, 240 K; 7, 272 K; 8, 294 K; 9, 300 K; 10, 350 K.

In order to establish the relative importance of the two routes for the oxidation of Ru^0 the infrared spectrum of adsorbed CO was also taken at low temperatures, between 120 and 350 K. As demonstrated in Fig. 10, adsorption of CO at 120 K produced intense absorption bands at 2180 and 2145 cm^{-1}, which disappeared during heating of the sample in the presence of CO up to about 240 K. This feature suggests that these bands belong to physisorbed CO (*17*). From among the CO bands discussed before only the LF band due to Ru_x–CO appeared at 120 K. However, with the rise in the temperature the HF and MF bands gradually developed from 170 K and they grew in intensity. As the dissociation of CO on Ru/Al_2O_3 can be excluded at such low temperatures we suggest that the dominant mode of oxidative disruption of Ru_x clusters involves CO and OH groups, and the route assisted by CO dissociation may contribute to this only above 300 K.

In the above considerations, as a starting basis we accepted the view that the HF and MF bands are due to the gem-dicarbonyl $Ru^I(CO)_2$ or $Ru^{n+}(CO)_2$ (*27–30, 32–36*) picture which has been strongly criticized recently by Chen *et al.* (*31*). We believe that our basic concept is still valid if we deny the existence of gem-dicarbonyl on Ru, as the findings of most of the previous works as well as the present study strongly support the idea that the HF and MF bands of adsorbed CO are to be attributed to CO bonded to positively charged Ru sites. After completion of this work two recent studies came to our attention. The interaction of CO with a stepped Ru single-crystal surface has been studied by pulsed field desorption mass spectrometry and the formation of subcarbonyl species $Ru(CO)_x^{n+}$ (x = 1–4, n = 1, 2) has been detected (*44*). The formation of gem-dicarbonyl has also been suggested in a NMR study of the CO–Ru/Al_2O_3 system (*45*).

3. Reductive Agglomeration of Ru^I Sites

An interesting feature of the interaction of CO with Rh/Al_2O_3 was that at higher temperatures the effect of CO was different: in this case, a gradual attenuation of the bands due to gem-dicarbonyl occurred, with simultaneous development of the spectral features of the Rh_x–CO species. A similar process for Ru/Al_2O_3 was clearly observed at around 498 K, where the HF and MF bands gradually attenuated (Figs. 5–6). The establishment of an intensification of the $\mathrm{Ru_x}$–CO band was not so easy, for, in contrast to the CO–Rh/$\mathrm{Al_2O_3}$ system, we could not produce HF and MF bands without a relatively intense LF band. In spite of this difficulty, an enhancement of the intensity of the LF band during depletion of the HF and MF bands in a certain case was clearly observed (Fig. 6). If we accept the assumption that the HF and MF bands are due to the $\mathrm{Ru^{I}(CO)_2}$ species, the above-mentioned spectral changes correspond to the transformation of gem-dicarbonyl, $\mathrm{Ru^{I}(CO)_2}$ to $\mathrm{Ru_x}$–CO species, or in other words to the reductive agglomeration of $\mathrm{Ru^{I}}$ to $\mathrm{Ru_x}$ clusters. The fact that the presence of $\mathrm{H_2}$ accelerates this process indicates the redox character of the surface process and further supports this conclusion.

As regards the effect of $\mathrm{H_2}$ on the reductive agglomeration of $\mathrm{Rh^{I}}$, several possibilities have been considered in our previous papers (*2*). The dominant effect is undoubtedly associated with the reducing effect of hydrogen activated on the metal and with its migration across the $\mathrm{Al_2O_3}$ surface. Evidence for the occurrence of the migration of hydrogen is provided by our earlier work on the $\mathrm{H_2} + \mathrm{CO_2}$ surface interaction on Ru/$\mathrm{Al_2O_3}$ (*21*) and also on Rh/$\mathrm{Al_2O_3}$ (*46, 47*), where extensive formation of formate on $\mathrm{Al_2O_3}$ was observed. This was explained by the activation of $\mathrm{H_2}$ on the metal and by a subsequent migration of activated hydrogen across the support surface and by its reaction with bicarbonate on $\mathrm{Al_2O_3}$ to yield the formate species.

Accordingly, the reductive agglomeration of $\mathrm{Ru^{I}}$ to $\mathrm{Ru_x}$ by CO can be described by the equation

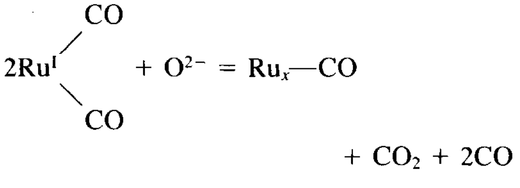

$$2\mathrm{Ru^{I}}\begin{array}{l}\diagup\mathrm{CO}\\ \diagdown\mathrm{CO}\end{array} + \mathrm{O^{2-}} = \mathrm{Ru_x{-}CO} + \mathrm{CO_2} + 2\mathrm{CO}$$

while the accelerating effect of $\mathrm{H_2}$ can be attributed to the reactions

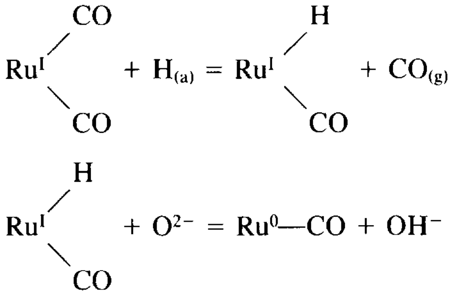

$$\mathrm{Ru^{I}}\begin{array}{l}\diagup\mathrm{CO}\\ \diagdown\mathrm{CO}\end{array} + \mathrm{H_{(a)}} = \mathrm{Ru^{I}}\begin{array}{l}\diagup\mathrm{H}\\ \diagdown\mathrm{CO}\end{array} + \mathrm{CO_{(g)}}$$

$$\mathrm{Ru^{I}}\begin{array}{l}\diagup\mathrm{H}\\ \diagdown\mathrm{CO}\end{array} + \mathrm{O^{2-}} = \mathrm{Ru^{0}{-}CO} + \mathrm{OH^-}$$

$$2\mathrm{Ru^{0}{-}CO} = \mathrm{Ru_x{-}CO} + \mathrm{CO_{(g)}} \quad (x = 2)$$

$$y\,\mathrm{Ru_x{-}CO} = \mathrm{Ru_{x,y}{-}CO} + (y - 1)\mathrm{CO}$$

REFERENCES

1. Solymosi, F., and Pásztor, M., *J. Phys. Chem.* **89,** 4783 (1985).

2. Solymosi, F., and Pásztor, M., *J. Phys. Chem.* **90,** 5312 (1986).

3. Primet, M., *J. Chem. Soc. Faraday Trans. I* **74,** 2570 (1978).

4. Primet, M., Védrine, J. C., and Naccache, G., *J. Mol. Catal.* **4,** 411 (1978).

5. Rice, C. A., Worley, S. D., Curtis, C. W., Guin, J. A., and Tarrer, A. R., *J. Chem. Phys.* **74,** 6748 (1981), and references therein.

6. Van 't Blik, H. F. J., van Zon, J. B. A., Huizinga, T., Vis, J. C., Koningsberger, D. C., and Prins, R., *J. Phys. Chem.* **87,** 2264 (1983).

7. Van 't Blik, H. F. J., van Zon, J. B. A. D., Huizinga, T., Vis, J. C., Koningsberger, D. C., and Prins, R., *J. Amer. Chem. Soc.* **107,** 3139 (1985).

8. Van 't Blik, H. F. J., van Zon, J. B. A. D., Koningsberger, D. C., and Prins, R., *J. Mol. Catal.* **25,** 379 (1984).

9. Bergeret, G., Gallezot, P., Gelin, P., Ben Taarit, Y., Lefebvre, F., Naccache, C., and Shannon, R. D., *J. Catal.* **104,** 279 (1987).

10. Zaki, M. J., Tesche, B., Kraus, L., and Knözinger, H., *Surf. Interface Anal.* **12,** 239 (1988).

11. Solymosi, F., Pásztor, M., and Rákhely, G., *J. Catal.* **110,** 413 (1988).

12. Dai, C. H., and Worley, S. D., *J. Phys. Chem.* **90,** 4219 (1986).

13. Solymosi, F., Bánsági, T., and Novák, É., *J. Catal.* **112,** 183 (1988).

14. Basu, P., Panayotov, D., and Yates, J. T., Jr., *J. Phys. Chem.* **91,** 3133 (1987).

15. Solymosi, F., and Pásztor, M., *J. Catal.* **104,** 312 (1987).

16. Solymosi, F., Novák, E., and Horváth, E., to be published.
17. Zaki, M. I., Kunzmann, G., Gates, B. C., and Knözinger, H., *J. Phys. Chem.* **91,** 2486 (1987).
18. Lynds, L., *Spectrochim. Acta* **20,** 1369 (1964).
19. Guerra, C. R., and Schulmann, J. H., *Surf. Sci.* **7,** 229 (1967).
20. Dalla Betta, R. A., *J. Phys. Chem.* **79,** 2519 (1975).
21. Solymosi, F., Erdöhelyi, A., and Kocsis, M., *J. Chem. Soc. Faraday Trans. 1* **77,** 1003 (1981).
22. Solymosi, F., and Raskó, J., *J. Catal.* **49,** 240 (1977).
23. Kobayashi, M., and Shirasaki, T., *J. Catal.* **28,** 289 (1973).
24. Goodwin, J. G., and Naccache, C., *J. Catal.* **64,** 482 (1980).
25. Brown, M. F., and Gonzalez, R. D., *J. Phys. Chem.* **80,** 1731 (1976).
26. Abbivantanaporn, P., and Gardner, R. A., *J. Catal.* **27,** 56 (1972).
27. Davydov, A. A., and Bell, A. T., *J. Catal.* **49,** 332 (1977).
28. Tamaru, K., "Proceedings, 7th International Congress on Catalysis Tokyo, 1980" (T. Seiyama and K. Tanabe, Eds.), p. 47. Elsevier, Amsterdam, 1981.
29. Xin Qin, Shi Xianxiang, Ying Pinliang, and Guo Xiexian, *React. Kinet. Catal. Lett.* **31,** 273 (1986).
30. Yamasaki, H., Kobori, Y., Noito, S., Onishi, T., and Tamaru, K., *J. Chem. Soc Faraday Trans. 1* **77,** 2913 (1981).
31. Hsiu-Wei Chen, Zheng Zhong, and White, J. M., *J. Catal.* **90,** 119 (1984).
32. Zecchina, A., Guglielminotti, E., Bossi, A., and Camia, M., *J. Catal.* **74,** 225 (1982).
33. Guglielminotti, E., Zecchina, A., Bossi, A., and Camia, M., *J. Catal.* **74,** 240 (1982).
34. Guglielminotti, F., Zecchina, A., Bossi, A., and Camia, M., *J. Catal.* **74,** 252 (1982).
35. Bossi, A., Carnisio, G., Garbassi, F., Giunchi, G., Petrini, G., and Zanderighi, L., *J. Catal.* **65,** 16 (1980).
36. Kunznetsov, V. L., Bell, A. T., and Yermakov, Y. J., *J. Catal.* **65,** 374 (1980).
37. Peri, J. B., and Hannan, R. B., *J. Phys. Chem.* **64,** 1526 (1960).
38. Knözinger, H., and Ratnasamy, P., *Catal. Rev. Sci. Eng.* **17,** 31 (1978).
39. Rákhely, G., and Solymosi, F., to be published.
40. Solymosi, F., and Erdöhelyi, A., *Surf. Sci.* **110,** L630 (1981).
41. Erdöhelyi, A., and Solymosi, F., *J. Catal.* **84,** 446 (1983).
42. Broden, G., Rhodin, T. N., Brucker, C., Benbow, G., and Hurych, Z., *Surf. Sci.* **59,** 593 (1976).
43. Kobori, Y., Naito, S., Onishi, T., and Tamaru, K., *J. Chem. Soc. Chem. Commun.,* 92 (1981).
44. Kruse, N., Abend, G., Chuah, G. K., and Block, J. H., private communication; Kruse, N., *Surf. Sci.* **178,** 820 (1986).
45. Root, T. W., and Duncam, T. M., paper presented at 10th North American Meeting of the Catalysis Society, San Diego, 1987. *J. Phys. Chem.* **92,** 4426 (1988).
46. Solymosi, F., Erdöhelyi, A., and Kocsis, M., *J. Catal.* **65,** 428 (1980).
47. Solymosi, F., Erdöhelyi, A., and Bánsági, T., *J. Chem. Soc. Faraday Trans. 1* **77,** 2645 (1981).